A&A 598, A128 (2017)
DOI: 10.1051/0004-6361/201629624

Astronomy & Astrophysics

The impact of the revised ^{17}O(p, α)^{14}N reaction rate on ^{17}O stellar abundances and yields

O. Straniero[1,2], C. G. Bruno[5], M. Aliotta[5], A. Best[6], A. Boeltzig[3], D. Bemmerer[4], C. Broggini[7], A. Caciolli[7,8], F. Cavanna[9], G. F. Ciani[3], P. Corvisiero[9], S. Cristallo[1,16], T. Davinson[5], R. Depalo[7,8], A. Di Leva[6], Z. Elekes[10], F. Ferraro[9], A. Formicola[2], Zs. Fülöp[10], G. Gervino[11], A. Guglielmetti[12], C. Gustavino[13], G. Gyürky[10], G. Imbriani[6], M. Junker[2], R. Menegazzo[7], V. Mossa[14], F. R. Pantaleo[14], D. Piatti[7,8], L. Piersanti[1,16], P. Prati[9], E. Samorjai[10], F. Strieder[15], T. Szücs[4], M. P. Takács[4], and D. Trezzi[11]

[1] INAF, Osservatorio Astronomico di Teramo, 64100 Teramo, Italy
e-mail: straniero@oa-teramo.inaf.it
[2] INFN, Laboratori Nazionali del Gran Sasso (LNGS), 67100 Assergi, Italy
[3] Gran Sasso Science Institute, INFN, Viale F. Crispi 7, 67100 L'Aquila, Italy
[4] Helmholtz-Zentrum Dresden-Rossendorf, Bautzner Landstr 400, 01328 Dresden, Germany
[5] SUPA, School of Physics and Astronomy, University of Edinburgh, EH9 3FD Edinburgh, UK
[6] Università di Napoli "Federico II" and INFN, Sezione di Napoli, 80126 Napoli, Italy
[7] INFN, Sezione di Padova, via Marzolo 8, 35131 Padova, Italy
[8] Department of Physics and Astronomy, University of Padova, via Marzolo 8, 35131 Padova, Italy
[9] Università degli Studi di Genova and INFN, Sezione di Genova, via Dodecaneso 33, 16146 Genova, Italy
[10] Institute for Nuclear Research (MTA ATOMKI), PO Box 51, 4001 Debrecen, Hungary
[11] Università degli Studi di Torino and INFN, Sezione di Torino, via P. Giuria 1, 10125 Torino, Italy
[12] Università degli Studi di Milano and INFN, Sezione di Milano, via G. Celoria 16, 20133 Milano, Italy
[13] INFN, Sezione di Roma La Sapienza, Piazzale A. Moro 2, 00185 Roma, Italy
[14] Università degli Studi di Bari and INFN, Sezione di Bari, 70125 Bari, Italy
[15] South Dakota School of Mines, 501 E. Saint Joseph St., SD 57701, USA
[16] INFN, Sezione di Perugia, 06123 Perugia, Italy

Received 31 August 2016 / Accepted 20 October 2016

ABSTRACT

Context. Material processed by the CNO cycle in stellar interiors is enriched in ^{17}O. When mixing processes from the stellar surface reach these layers, as occurs when stars become red giants and undergo the first dredge up, the abundance of ^{17}O increases. Such an occurrence explains the drop of the ^{16}O/^{17}O observed in RGB stars with mass larger than ~1.5 $M_\odot$. As a consequence, the interstellar medium is continuously polluted by the wind of evolved stars enriched in ^{17}O.
Aims. Recently, the Laboratory for Underground Nuclear Astrophysics (LUNA) collaboration released an improved rate of the ^{17}O(p, α)^{14}N reaction. In this paper we discuss the impact that the revised rate has on the ^{16}O/^{17}O ratio at the stellar surface and on ^{17}O stellar yields.
Methods. We computed stellar models of initial mass between 1 and 20 $M_\odot$ and compared the results obtained by adopting the revised rate of the ^{17}O(p, α)^{14}N to those obtained using previous rates.
Results. The post-first dredge up ^{16}O/^{17}O ratios are about 20% larger than previously obtained. Negligible variations are found in the case of the second and the third dredge up. In spite of the larger ^{17}O(p, α)^{14}N rate, we confirm previous claims that an extra-mixing process on the red giant branch, commonly invoked to explain the low carbon isotopic ratio observed in bright low-mass giant stars, marginally affects the ^{16}O/^{17}O ratio. Possible effects on AGB extra-mixing episodes are also discussed. As a whole, a substantial reduction of ^{17}O stellar yields is found. In particular, the net yield of stars with mass ranging between 2 and 20 $M_\odot$ is 15 to 40% smaller than previously estimated.
Conclusions. The revision of the ^{17}O(p, α)^{14}N rate has a major impact on the interpretation of the ^{16}O/^{17}O observed in evolved giants, in stardust grains and on the ^{17}O stellar yields.

Key words. nuclear reactions, nucleosynthesis, abundances – stars: abundances – stars: evolution

1. Introduction

The two lighter oxygen isotopes participate in the NO section of the CNO cycle. When CNO reaches an equilibrium, as occurs in the H-burning shell of a giant star or in the central region of main-sequence stars, the ^{16}O/^{17}O ratio is simply given by the inverse ratio of the respective proton-capture reaction rates,

$$\frac{^{16}\mathrm{O}}{^{17}\mathrm{O}} = \frac{(\langle\sigma v\rangle_{^{17}\mathrm{O(p,\gamma)}^{18}\mathrm{F}} + \langle\sigma v\rangle_{^{17}\mathrm{O(p,\alpha)}^{14}\mathrm{N}})}{\langle\sigma v\rangle_{^{16}\mathrm{O(p,\gamma)}^{17}\mathrm{F}}}. \quad (1)$$

In practice, since the three reaction rates only depend on temperature, this isotopic ratio traces the temperature profile within the

H-burning zone. Variations of the $^{16}O/^{17}O$ isotopic ratio appear at the surface when the ashes of the H burning are mixed with the stellar surface as a result of, for instance, convective instabilities affecting the stellar envelope in red giant (RGB) and asymptotic giant (AGB) stars. This isotopic ratio can be measured from the IR spectra of giant stars. In early studies, the CO vibration-rotation, 4.6 μm fundamental or 2.3 μm first overtone bands were commonly used (Harris et al. 1988; Smith & Lambert 1990). With the advent of IR spectrographs characterized by high dispersion and high signal-to-noise ratios, more lines in the near-IR spectrum can be exploited to derive the CNO isotopic composition of giant stars (García-Hernández et al. 2010; Abia et al. 2012; Lebzelter et al. 2015; Hinkle et al. 2016). These measurements allow us to probe the depth attained by the mixing episodes that are responsible for the chemical variations observed at the stellar surface. We recall that in addition to convection, other processes may induce or contribute to deep mixing episodes, such as rotation, magnetic buoyancy, gravity waves, and thermohaline circulation (Dearborn 1992; Boothroyd et al. 1994; El Eid 1994; Charbonnel 1995; Nollett et al. 2003; Denissenkov & Tout 2003; Busso et al. 2007; Eggleton et al. 2008; Palmerini et al. 2011). In all cases, the reliability of the deep mixing probe depends on our knowledge of the rates of the nuclear reactions determining the $^{16}O/^{17}O$ ratio in the H-burning regions, i.e, $^{16}O(p,\gamma)^{17}F$, $^{17}O(p,\gamma)^{18}F$ and $^{17}O(p,\alpha)^{14}N$. The last two reactions have recently been studied by the LUNA collaboration (Scott et al. 2012; Di Leva et al. 2014; Bruno et al. 2016) to obtain precise underground measurements of their cross sections at relatively low energy. At variance with the (p,γ) channel, for which negligible variations with respect to previous investigations have been found, the (p,α) rate has been substantially revised. The latter reaction is the main destruction channel of ^{17}O. Thanks to the significant background reduction of the underground laboratory, a new direct determination of the 64.5 keV resonance strength has led to the most accurate value to date, $\omega\gamma = 10.0\pm1.4_{stat}(\pm0.7_{syst})$ neV. The 64.5 keV resonance dominates the reaction rate for temperatures below 100 MK. The (bare) proton partial width of the corresponding state at $E_X = 5672$ keV in ^{18}F is $\Gamma_p = 35 \pm 5_{stat}(\pm3_{syst})$ neV, which is about a factor of two higher than previously claimed. As a consequence, the $^{17}O(p,\alpha)^{14}N$ reaction rate in the temperature range most relevant for the hydrostatic H burning, $20 < T/MK < 100$, is about a factor of two higher than previously estimated. Larger temperatures may be attained in explosive H burning, such as in the case of nova events (Di Leva et al. 2014), and in the hot bottom burning (HBB) process occurring in super-AGB stars (Siess 2010; Ventura et al. 2012; Doherty et al. 2014). For $T >$ 100 MK, however, the influence of the 64.5 keV resonance on the total reaction rate is negligible. In Fig. 1, the corresponding variation of the equilibrium value of $^{16}O/^{17}O$ (Eq. (1)) as function of the temperature is compared to those obtained by adopting the $^{17}O(p,\alpha)^{14}N$ rates reported in the popular compilations NACRE (Angulo et al. 1999) and STARLIB (Iliadis et al. 2010; Buckner et al. 2015). As is immediately seen, the revision of the $^{17}O(p,\alpha)^{14}N$ rate implies equilibrium values of the $^{16}O/^{17}O$ ratio, which are up to a factor of 2 larger than those obtained so far.

In this paper we discuss the expected variations of the $^{16}O/^{17}O$ at the surface of stars with different masses. In particular, we consider the effects induced by the major deep mixing episodes, such as the dredge-up events and the extra-mixing process that is likely operating in bright low-mass RGB stars and, perhaps, also during the AGB phase. We do not address here the impact on the HBB, which is an important nucleosynthesis episode occurring in massive AGB stars. Because of the complexity of this phenomenon, which is largely not yet fully understood, we decided to dedicate a companion paper to the discussion of the impact of the revised $^{17}O(p,\alpha)^{14}N$ rate on the HBB (Lugaro et al. 2017).

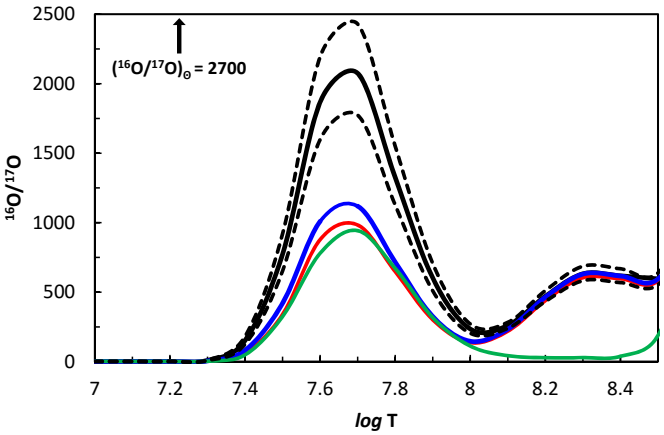

Fig. 1. Equilibrium values of the $^{16}O/^{17}O$ vs. temperature (see Eq. (1)). The black curve was obtained by adopting the revised rate of the $^{17}O(p,\alpha)^{14}N$ reaction (median values of Bruno et al. 2016) and the two black dashed lines show the recommended maximum and minimum values compatible with the experimental data, which corresponds to the 1σ error bar of the measured nuclear cross section. For comparisons, the blue, red, and green lines show the results obtained by adopting the $^{17}O(p,\alpha)^{14}N$ rate from Buckner et al. (2015), Iliadis et al. (2010), and Angulo et al. (1999), respectively.

A variation of the stellar ^{17}O yields is also expected. According to the extant chemical evolution models (see, for example, the recent review of Nittler & Gaidos 2012; or CGE models discussed in Prantzos et al. 1996; Romano & Matteucci 2003; Kobayashi et al. 2011), the average ^{17}O abundance in the interstellar medium (ISM) should increase with time, mainly because of the ejecta of intermediate and massive stars. We show that with the revision of the $^{17}O(p,\alpha)^{14}N$ reaction rate, the ^{17}O yields are substantially reduced. As a consequence, the rate of growth of the ^{17}O in the ISM should be slower than previously estimated.

We computed all the stellar models presented in this paper by means of the latest release of the full-network stellar evolution code (FUNS, Straniero et al. 2006; Piersanti et al. 2013). Except for the $^{17}O(p,\alpha)^{14}N$, all the rates of the other reactions involved in the H burning are from Adelberger et al. (2011). When not specified, the initial composition of the models is solar (Lodders et al. 2009). It implies $Z = 0.014$ and $Y = 0.27$. The various uncertainties affecting stellar models and the related nucleosynthesis results, including those due to the treatment of mixing, are discussed in some detail in Sect. 2 of Straniero et al. (2014; see also Sects. 4 and 5 in Lebzelter et al. 2015). More details on the theoretical estimation of the O isotopic ratios can be found in several papers, including Dearborn (1992), Boothroyd et al. (1994), El Eid (1994), Stoesz & Herwig (2003), Karakas & Lattanzio (2014), Halabi & Eid (2015). We used the same stellar evolution code (FUNS) as in Cristallo et al. (2015). Nevertheless, the ^{17}O abundances and yields presented in this paper slightly differ from the corresponding values reported in the full-network repository of updated isotopic tables & yields (FRUITY) because we updated the initial composition (Lodders et al. 2009; instead of Lodders 2003) and several reaction rates, in particular, those of the CNO cycle.

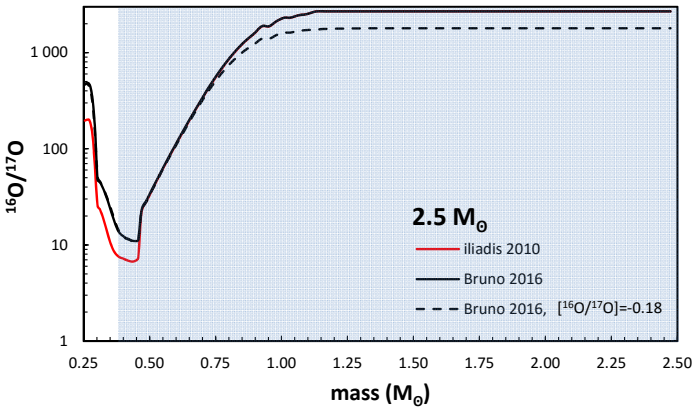

Fig. 2. Oxygen isotopic ratio in the H-rich envelope of a 2.5 $M_\odot$ newborn red giant star, just before the occurrence of the FDU. The models were computed with different $^{17}O(p,\alpha)^{14}N$ reaction rates and/or different initial compositions (see the legend). The shaded area shows the portion of the stellar envelope that are mixed at the time of the FDU.

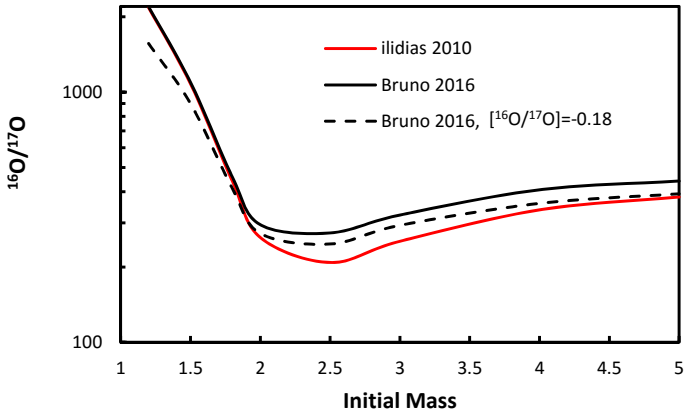

Fig. 3. Post-FDU $^{16}O/^{17}O$ at the surface of models with different initial mass and different rates and/or initial composition (see the legend).

2. Low- and intermediate-mass stars

In this section we discuss the variations of the $^{16}O/^{17}O$ predicted by models of low- and intermediate-mass stars after the major dredge-up episodes, as due to the revision of the $^{17}O(p,\alpha)^{14}N$ reaction rate. The possible effects on low-mass stars undergoing RGB or AGB extra-mixing episodes are also discussed.

2.1. The first dredge up

The first appearance at the surface of a star of the chemical variations caused by the internal nucleosynthesis occurs just after the exhaustion of the central hydrogen when the star leaves the main sequence to become a red giant. A convective instability develops in the most external layers and quickly extends down to the region where the H burning took place. This is the so-called first dredge up (FDU).

The solar value of the $^{16}O/^{17}O$ is 2700 (Lodders et al. 2009). Models of intermediate-mass stars ($2 < M/M_\odot < 8$) show that after the FDU this isotopic ratio is reduced down to values between 200 and 500, depending on the initial mass and composition, essentially because of ^{17}O production. In more detail, these stars develop a rather extended convective core at the onset of the core H burning, corresponding to the main sequence of the HR diagram. The central (maximum) temperature is typically between 20 and 30 MK and the corresponding equilibrium value of the $^{16}O/^{17}O$ ratio (<100) is established in the whole convective core. Later on, at the epoch of the FDU, the external convective instability penetrates the portion of the core that was efficiently mixed when the star was on the main sequence. As a consequence, the surface abundance of ^{17}O increases, while that of ^{16}O slightly decreases.

In Fig. 2 we plot the $^{16}O/^{17}O$ profile within the H-rich envelope of a newborn giant star with 2.5 $M_\odot$ and solar metallicity. The three compositional profiles, which are all sampled just before the onset of the FDU, were obtained under different assumptions for the $^{17}O(p,\alpha)^{14}N$ reaction rate and/or different initial composition: the Iliadis et al. (2010) rate and solar $^{16}O/^{17}O$ (red line), the new rate (median values of Bruno et al. 2016) and solar $^{16}O/^{17}O$ (black line), and the new rate and $^{16}O/^{17}O$ lower than solar (black dashed line). This figure clearly shows that in the most internal region of the envelope, where the H burning attained the CNO equilibrium, the $^{16}O/^{17}O$ does not depend on the initial composition, but is fixed by the production and destruction rates of the ^{17}O (Eq. (1) and Fig. 1). Therefore, the abundance ratio in the deepest layer of the H-rich envelope of a giant star only depends on the reaction rates and on the maximum temperature previously experienced. On the contrary, the O isotopic ratio in the external envelope reflects the initial composition. Later on, the external convection penetrates the internal region, modifying the surface composition. The shaded area in Fig. 2 shows the region that is mixed by the convective instability at the epoch of the FDU.

The maximum temperature attained in the deepest layer reached by the FDU varies with the initial stellar mass and composition. For a fixed chemical composition (same initial helium and metallicity), the larger the stellar mass the larger the temperature at the innermost convective boundary. In contrast, the ashes of the H burning are mixed with the material in the cooler external envelope with the initial composition and the larger the envelope mass the smaller the variation of the composition at the stellar surface. The combination of these two effects leads to the plots reported in Fig. 3, in which we show the surface value of the $^{16}O/^{17}O$ ratio after the FDU versus the initial stellar mass. For convenience, the values of the post-FDU $^{16}O/^{17}O$ are listed in Table 1. In all cases, a sharp decrease of the $^{16}O/^{17}O$ ratio is found for $1.2 < M/M_\odot < 2.5$, followed by a shallower increase for more massive stars. In low-mass stars ($M < 1.2\ M_\odot$), the convective core disappears at the onset of the main sequence. In that case the $^{16}O/^{17}O$ does not change after the FDU.

The maximum difference of 20% between models, which are obtained with the old and new ^{17}O destruction rates, is found at $M = 2.5\ M_\odot$. The change implied by the new rate may be compensated by varying the initial O composition (dashed line in Fig. 3).

2.2. The second and third dredge up

During the early-AGB phase, intermediate-mass stars ($M \geq 4\ M_\odot$) experience a second dredge-up episode. This episode occurs when the H-burning shell is temporarily switched off and the convective envelope can penetrate the H-exhausted core. In this case, H-depleted material enriched with the ashes of the H-burning is brought to the surface. At variance with the FDU, the change of the $^{16}O/^{17}O$ at the surface of the star is small. The situation is illustrated in Fig. 4: in the upper panel we show the evolution of the $^{16}O/^{17}O$ at the surface of a 6 $M_\odot$ model (solar initial composition) up to the early-AGB phase, while in

Table 1. Post-FDU $^{16}O/^{17}O$ values.

$M/M_\odot$ initial	I2010[a] 2696	LUNA[b] 2696	LUNA[c] 1797
1.2	2177	2195	1564
1.5	1081	1096	901
1.8	440	458	412
2.0	262	295	272
2.5	208	274	247
3.0	253	323	294
4.0	338	407	359
5.0	381	441	392

Notes. [(a)] $^{17}O(p,\alpha)^{14}N$ from Iliadis et al. (2010), solar initial composition; [(b)] $^{17}O(p,\alpha)^{14}N$ from Bruno et al. (2016), solar initial composition; [(c)] $^{17}O(p,\alpha)^{14}N$ from Bruno et al. (2016), and initial $[^{16}O/^{17}O] = -0.18$.

the lower panel we report the evolutions of the corresponding mass fractions of ^{16}O (solid) and ^{17}O (dotted). The red lines refer to the models calculated by adopting the Iliadis et al. (2010) rate for the $^{17}O(p,\alpha)^{14}N$ reaction, while the black lines represent models obtained with the new LUNA rate. In both cases the variations at the stellar surface are largely dominated by the large increase of the ^{17}O abundance caused by the FDU. Later on, the H burning restarts whereas the He-burning shell periodically undergoes recursive thermonuclear runaways (i.e., thermal pulses; TP). Then, third-dredge-up episodes occur after each thermal pulse, except for the first and a few final TPs. As for the second dredge up, the convective envelope penetrates the H-exhausted core. However, the variation of the O isotopic ratio caused by the third dredge up is generally small. An increase of the $^{16}O/^{17}O$ is actually found in low metallicity models owing to the dredge up of primary ^{16}O produced by the He burning (see, for example, O abundances listed in the FRUITY database Cristallo et al. 2015), but this phenomenon is independent of the adopted CNO reaction rates.

2.3. Extra mixing in RGB and AGB stars

It is generally accepted that the FDU alone cannot account for the CNO abundances measured in the brightest RGB stars with $M < 2\ M_\odot$ and that an extra-mixing process should be at work in the upper RGB (Charbonnel 1995). In particular, the $^{12}C/^{13}C$ ratio in these stars is substantially lower than predicted by stellar models after the occurrence of the FDU. On the contrary, model predictions are in good agreement with the C isotopic ratios measured in more massive RGB stars as well as in faint RGB stars with low mass. For instance, values of $^{12}C/^{13}C < 20$ are commonly found in low-mass RGB stars that are brighter than the so-called RGB bump, i.e., the peak in the RGB luminosity function due to the temporary stop of the luminosity growth that occurs when the H-burning shell approaches the chemical discontinuity left by the FDU (Gilroy & Brown 1991; Gratton et al. 2000; Abia et al. 2012). In contrast, model predictions for the $^{12}C/^{13}C$ ratio after the FDU are always >20. In principle, the O isotopic ratios may also be affected by the extra mixing, although there is some observational evidence against such a possibility (Abia et al. 2012). In this context, the new (stronger) rate of the $^{17}O(p,\alpha)^{14}N$ reaction can affect the variation of the ^{17}O at the stellar surface. In Fig. 5 we report C and O isotopic ratios in the innermost layers of the H-rich envelope of a RGB-bump model with initial mass 1.5 $M_\odot$ and initial solar composition.

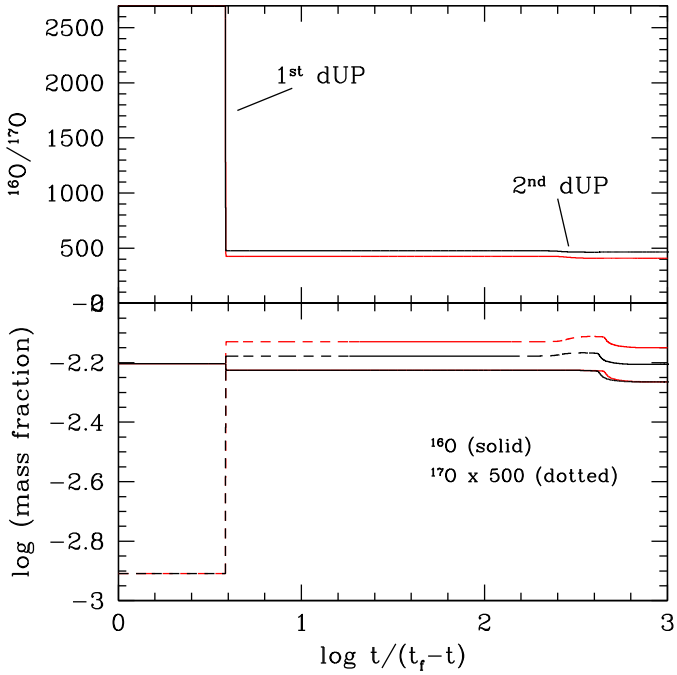

Fig. 4. Evolution of the two lighter oxygen isotopes in a 6 $M_\odot$ model (solar initial composition). *Upper panel*: $^{16}O/^{17}O$ ratio. *Lower panel*: ^{16}O (solid) and ^{17}O (dotted). Red lines refer to the models calculated by adopting the Iliadis et al. (2010) rate for the $^{17}O(p,\alpha)^{14}N$ reaction, while black lines represent models obtained with the new LUNA rate (Bruno et al. 2016). $t_f = 68$ Myr corresponds to the age of the last computed model (end of the early AGB).

Sizeble variations of C, N, and O isotopes, as due to H burning, occur at $m \leq 0.277\ M_\odot$. Since the internal boundary of the convective envelope is at $m = 0.292\ M_\odot$, extra mixing is needed to bring the product of the CNO nucleosynthesis into the convective zone. In the same figure, the temperature profile is also reported (red line). A modification of the $^{16}O/^{17}O$ ratio would require a much deeper extra mixing than that needed to explain the C isotopic ratio commonly observed in bright low-mass RGB stars.

Since the actual physical process that is capable of driving an efficient mixing below the convective envelope in giant stars is still largely unknown, a few free parameters are usually introduced to investigate the effects of these phenomena. We do not pretend to discuss these effects or even the nature of the extra-mixing processes. Several paper have been already dedicated to this subject (see, e.g., Dearborn 1992; Boothroyd et al. 1994; El Eid 1994; Charbonnel 1995; Nollett et al. 2003; Denissenkov & Tout 2003; Busso et al. 2007; Eggleton et al. 2008; Charbonnel & Lagarde 2010; Palmerini et al. 2011, and references therein). The models presented here just aim to highlight possible effects of the revised $^{17}O(p,\alpha)^{14}N$ rate. Starting from the RGB-bump model shown in Fig. 5, we switched on an artificial extra-mixing process extending from the convective boundary down to a maximum temperature T_{max}. We set the mixing velocity to 100 cm/s, which is about 2 orders of magnitude slower than that in the convective region. Mixing velocities of this order of magnitude are expected in the case of thermohaline mixing (Charbonnel & Zahn 2007) and magnetic buoyancy (Palmerini et al. 2009), while somewhat lower values have been estimated for rotation induced mixing (Palacios et al. 2006). We verified that the C and O isotopic ratios at the stellar surface does not substantially depend on the assumed mixing velocity,

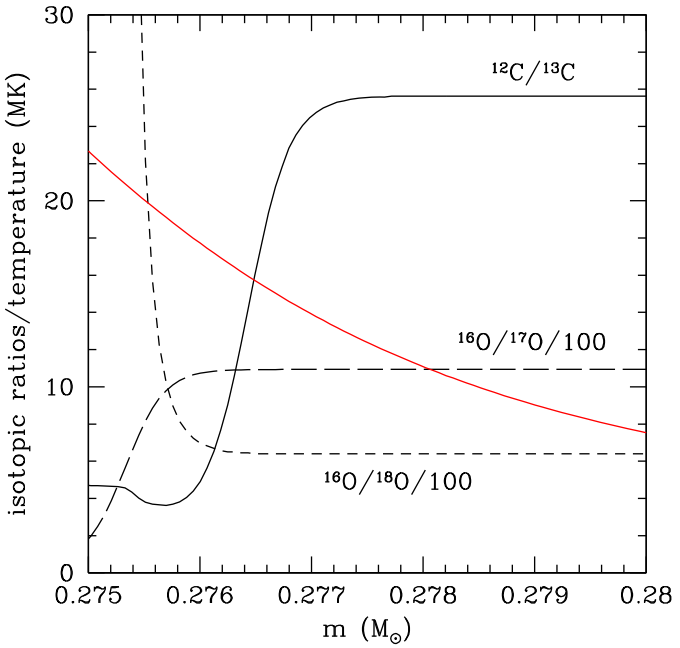

Fig. 5. C and O isotopic ratios in the innermost portion of the H-rich envelope of a RGB-bump model with $M = 1.5\ M_\odot$ (solar initial composition): $^{12}C/^{13}C$ (black solid line), $^{16}O/^{17}O$ (short dashed line), and $^{16}O/^{18}O$ (long dashed line). The red line represents the temperature profile (in MK).

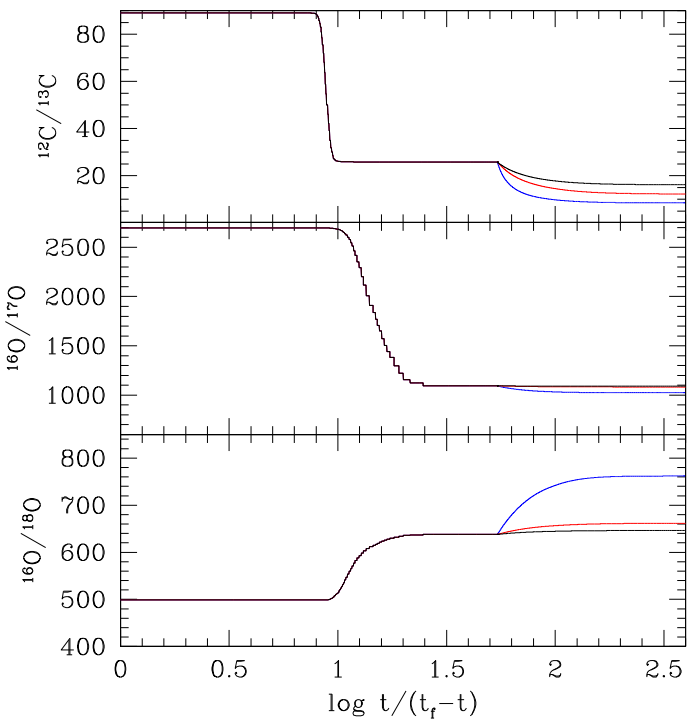

Fig. 6. Evolution up to the RGB tip of C and O isotopic ratios in the 3 models with extra mixing described in the text. The maximum temperature attained by extra mixing is $T_{max} = 20$, 21, and 23 MK (black, red, and blue lines, respectively). In all cases, the fluid velocity in the extra-mixing zone is about 1/100 of that in the fully convective envelope. The evolutionary timescale has been properly rescaled to $t_f = 2.91$ Gyr, which corresponds to the onset of the core-He burning. The FDU starts at $\log t/(t - t_f) \sim 1$, while the extra-mixing process is activated just after $\log t/(t - t_f) \sim 1.7$, namely, the epoch of the RGB bump.

but depends mainly on T_{max}. In Fig. 6 we show the evolution of the C and O isotopic ratios for $T_{max} = 20$, 21, and 23 MK. The most extreme case implies an extra-mixing zone extending from the internal convective boundary down to the outer border of the H-exhausted core. After the activation of the extra mixing, in all three cases the $^{12}C/^{13}C$ quickly drops below 20. The resulting C isotopic ratios are in good agreement with the observed values for the brightest low-mass RGB stars. In contrast, one only finds a non-negligible enhancement of the $^{16}O/^{18}O$ in the most extreme case, whilst in spite of the stronger rate of the $^{17}O(p,\alpha)^{14}N$ reaction, the $^{16}O/^{17}O$ practically remains unchanged.

In principle, even hotter regions may be attained by an AGB extra mixing. However, the actual occurrence of this process is still largely debated (see, for example, Lebzelter et al. 2008; Lederer et al. 2009; Karakas et al. 2010; Busso et al. 2010; Stancliffe 2010). Nevertheless, in order to investigate the effects of the revised rate of the $^{17}O(p,\alpha)^{14}N$ reaction on the O isotopes of AGB stars possibly undergoing extra mixing, we extended the computation of the 2 $M_\odot$ model up to the AGB tip. An AGB extra mixing extending down to $T_{max} = 40$ MK was activated since the first termal pulse. In addition, a RGB extra mixing ($T_{max} = 22$ MK) was also activated after the occurrence of the RGB bump. In both cases the average fluid velocity in the extra-mixing zone was set to 100 cm/s. The result is shown in Fig. 7. The $^{16}O/^{17}O$ should increase in the case of an AGB extra mixing, contrary to the variations induced by the FDU and, to a lesser extent, by the RGB extra mixing. The reason for this increase is simple: after the FDU, the $^{16}O/^{17}O$ drops down to ~300, while at $T = 40$ MK the equilibrium value of this ratio is ~1870 (see Fig. 1). Therefore, as a consequence of the AGB extra mixing, the material with high $^{16}O/^{17}O$ of the most internal portion of the H-burning shell is mixed with the envelope material that is characterized by low $^{16}O/^{17}O$. This effect is weaker for stars with smaller initial mass because the $^{16}O/^{17}O$ after the FDU is higher (see Fig. 3). With previous $^{17}O(p,\alpha)^{14}N$ reaction rates (e.g., Iliadis et al. 2010), the equilibrium values of the $^{16}O/^{17}O$ would be a factor of two smaller, thus reducing the overall increase of this isotopic ratio at the stellar surface. As a whole, in spite of the larger $^{17}O(p,\alpha)^{14}N$ rate, the variation of $^{16}O/^{17}O$ caused by the AGB extra mixing is much smaller than those of the other CNO isotopic ratios, such as $^{12}C/^{13}C$, $^{14}N/^{15}N$, and $^{16}O/^{18}O$. At the beginning of the C-star phase, i.e., when C/O = 1, $^{16}O/^{17}O$ is ~400, which is a 30% larger than the value obtained with the rate provided by Iliadis et al. (2010). We note that C stars affected by AGB extra mixing should show extreme values of $^{14}N/^{15}N$ ($>2\times10^4$) and $^{16}O/^{18}O$ ($>2\times10^3$), while the $^{12}C/^{13}C$ should be ≤20.

3. Yields

Oxygen-17 is a secondary product of the H burning and, therefore, all stars contribute to its synthesis. The major contribution to the pollution of the interstellar medium likely comes from massive stars ($M > 10\ M_\odot$). The winds of red giant stars of intermediate and low mass provide further contributions on a longer timescale. Extant chemical evolution models show that the abundance of ^{17}O in the ISM of the galactic disk increases with time (see the review of Nittler & Gaidos 2012, and references therein). This expectation is substantially confirmed by the abundance analysis of stars belonging to stellar populations of different ages and in the ISM (see, e.g., Nittler & Gaidos 2012; Lebzelter et al. 2015). The ^{17}O increase with time is stronger toward the Galactic center than in the outermost regions because

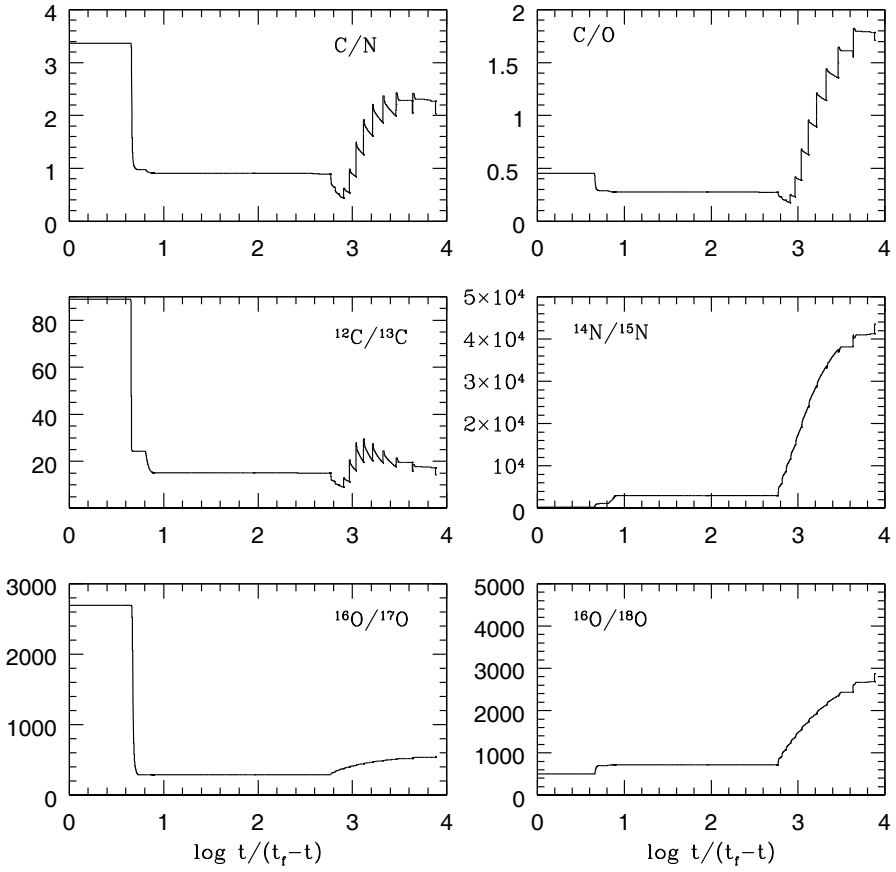

Fig. 7. Evolution up to the AGB tip of C, N, and O elemental and isotopic ratios in a 2 $M_\odot$ model with both RGB and AGB extra mixing. In the first case the maximum temperature was fixed to T_{max} = 22 MK, while in the latter T_{max} = 40 MK (see text for further details). The evolutionary timescale was rescaled to t_f = 1.196 Gyr, which corresponds to the age of the last computed model (AGB tip). The FDU occurs at $\log t/(t - t_f) \sim 0.7$, while some effect of the RGB extra mixing is visible a bit later. Finally the combined actions of the and the AGB extra mixing arise at $\log t/(t - t_f) > 2.8$.

of the increase of the stellar density at short Galactic radius and the consequent increase of the pollution rate (see Figs. 1 and 2 in Nittler & Gaidos 2012). Extant nucleosynthesis models show that stars with mass between 2 and 20 $M_\odot$ should release a few 10^{-5} $M_\odot$ of ^{17}O. Because ^{17}O is a secondary isotope, its production is higher at larger metallicity. More precisely, the yield depends on the initial C+N+O abundance.

As for intermediate-mass stars, in models of massive stars the amount of ^{17}O in the envelope is also enhanced as a consequence of the FDU. Here, we refer to the progenitors of type II supernova, which retain a H-rich envelope up to the final explosion. On the contrary, the ^{17}O is destroyed in the H-exhausted core. Then, the ^{17}O in the envelope remains unchanged after the FDU and until the core collapse. Also the final explosion does not affect the ^{17}O yield; see, e.g., Limongi et al. (2000, 2001), where both pre- and post-explosive yields are discussed, or Kobayashi et al. (2011), where it is shown that the ^{17}O yield does not depend on the explosion energy. Indeed, the H-rich envelope expands prior to the passage of the shock wave, so that the explosive nucleosynthesis is inhibited. In practice, a reasonable estimation of the ^{17}O yield could be obtained by multiplying the ^{17}O mass fraction after the FDU by the total mass of H-rich material ejected during the long hydrostatic evolution (by stellar wind) or as a consequence of the final explosion. Therefore, the adopted mass loss rate after the FDU, and the details of the final explosion, are not critical to modeling the ^{17}O yield in massive stars. This approximation is reasonable for most massive stars, except in the case of an early ejection of the whole envelope that stops the growth of the H-exhausted core, as occurs in Wolf-Rayet stars. In contrast, there is a major uncertainty because of the formation of a semi-convective shell instability during the core H burning, when the fully convective core recedes and leaves a decreasing H profile. As is well known, depending on the adopted mixing scheme, the core He burning may start when the star is still a blue compact structure or after it has expanded and become a red giant (see, e.g., Langer & Maeder 1995, Fig. 3, in particular). In the former case, the occurrence of the FDU is delayed; more precisely, it occurs after the end of the core-He burning. In this case the amount of H-rich material lost before the FDU may be greater and, therefore, the total yield is smaller.

In the models of massive stars presented here, we adopted a semi-convective scheme, i.e., the degree of mixing is calibrated in order to establish convective neutrality[1] in the whole semi-convective layer. In this case the mixing efficiency is substantially limited, so that the FDU occurs soon after the main-sequence phase. As a result, most of the envelope mass is lost after the occurrence of the FDU. Then, we computed three models with solar initial composition and masses 12, 15, and 20 $M_\odot$, which are representative of the most common type II supernova progenitors. We stopped the computation at the end of the C-burning phase. At that time, the residual stellar lifetime is so short that the composition of the H-rich envelope and the H-exhausted core mass remain frozen up to the final explosion. Therefore, we obtained the total yield by adding the ^{17}O mass contained in the H-rich envelope of the last computed model to the amount of ^{17}O cumulatively ejected before the end of the C-burning phase.

The resulting yields are reported in Table 2; they are net yields, namely the difference between the ^{17}O mass ejected during the whole stellar lifetime and the initial total ^{17}O mass. Results for different ^{17}O(p, α)^{14}N reaction rates are provided in

[1] $\nabla_{adiabatic} - \nabla_{radiative} = 0$, where $\nabla = \frac{\partial \ln T}{\partial \ln P}$.

Table 2. ^{17}O yields.

M	I2010[a]	LUNA[b]	Var (%)
1.5	0.16	0.17	–1
2.5	4.78	3.57	–22
4	5.08	4.19	–15
6	5.70	4.70	–17
12	5.95	4.70	–21
15	4.42	3.52	–20
20	2.38	1.38	–42

Notes. Net yields are listed in 10^{-5} $M_\odot$; [(a)] $^{17}O(p,\alpha)^{14}N$ from Iliadis et al. (2010), solar initial composition; [(b)] $^{17}O(p,\alpha)^{14}N$ from Bruno et al. (2016), and solar initial composition.

Cols. 2 and 3. Once the different initial compositions and reaction rate libraries are considered, the yields listed in Col. 2 are in good agreement with those reported by Kobayashi et al. (2011) and Chieffi & Limongi (2013; non-rotating models). Yields of a selected sample of low- and intermediate-mass stellar models with solar composition, as described in the previous sections, are reported as well. In this case all the models were evolved up to the AGB tip and no extra-mixing processes were included.

The new LUNA rate implies a sizeable reduction of the net yield of ^{17}O of up to a 40%. This result is almost independent of the initial metallicity or He content. The impact on models of Galactic chemical evolution deserves further investigation. In particular, we expect a slower rate of ^{17}O pollution of the ISM (see the discussion in Sect. 4).

4. Conclusions

We have revised the theoretical predictions of the $^{16}O/^{17}O$ ratios and of the ^{17}O yields from stars in a wide range of initial masses. We based all the computations on the new recommended values of the $^{17}O(p,\alpha)^{14}N$ reaction rate as described by Bruno et al. (2016). Bruno et al. (2016) also provide an upper and a lower limit for this reaction. As seen in Fig. 1, the $^{16}O/^{17}O$ values found using rates from previous compilations are outside the updated error band. Similarly, the uncertainty implied for the ^{17}O yields is much smaller than the difference between the revised values and the previous evaluations.

Reaction rates with uncertainties at the level of a 20% (or lower), as recently achieved by the LUNA collaboration for the $^{17}O(p,\alpha)^{14}N$ and $^{17}O(p,\gamma)^{18}F$ reactions, are required to constrain the efficiency of the various deep-mixing episodes operating in stars of various masses. Thanks to the improved accuracy of the relevant reaction rates, it will become possible to check the reliability of the numerical algorithms used to model stellar convection and other dynamical and secular instabilities in stellar interiors. In this context, comparisons of model predictions with $^{16}O/^{17}O$ ratios in giant stars is of primary importance, providing calibration tools for the various free parameters whose values are not fixed by the theory. Similarly, O-rich, pre-solar grains may also provide useful constraints for the models (Lugaro et al. 2017). The revision of the ^{17}O yields could have a major impact on Galactic chemical evolution studies. In particular it should help the interpretation of the oxygen isotopic composition of various Galactic components, such the Sun, giant stars, and diffused matter. In this context, Lebzelter et al. (2015), analyzing post-FDU measurements of the O isotopic ratios in RGB stars belonging to Galactic open clusters, conclude that the O isotopic composition of the Sun does not represent the original composition of the gas from which these stars formed. In particular, they were able to reproduce the observed O abundance by assuming smaller-than-solar initial O isotopic ratios. Possibly, this occurrence may be explained in the framework of Galactic chemical evolution. Indeed, as shown by, for example, Prantzos et al. (1996), Romano & Matteucci (2003), Kobayashi et al. (2011), Nittler & Gaidos (2012), the $^{16}O/^{17}O$ ratio decreases with time, so that stars that are younger than the Sun should have been formed, on the average, from a gas characterized by smaller oxygen isotopic ratios. Models obtained with the new and higher rate of the $^{17}O(p,\alpha)^{14}N$ reaction, which implies larger $^{16}O/^{17}O$ after the FDU, confirm and even reinforce the need of smaller-than-solar initial $^{16}O/^{17}O$ to reproduce the ratios observed in post-FDU giants belonging to Galactic open clusters. For instance, we obtained the models represented with dashed lines in both Figs. 2 and 3 by assuming an initial $^{16}O/^{17}O = 1797$; this value is lower than the solar value (2700) and roughly corresponds to the weighted average $^{16}O/^{17}O$ ratio of the interstellar medium in the region of the Galactic disk closer to the Sun (between 6 and 10 kpc from the Galactic center), as derived from measurements of CO molecular lines (Wouterloot et al. 2008; see also Penzias 1981). On the other hand, Kobayashi et al. (2011) found that their GCE model underestimates the solar $^{16}O/^{17}O$ and conclude that a reduction of the ^{17}O yields could solve this problem. As shown in Sect. 3, the revision of the $^{17}O(p,\alpha)^{14}N$ reaction rate goes in this direction and, therefore, it could alleviate the problem.

As a whole, more stringent constraints to important phenomena, such as stellar migration or the observed composition gradients along the Galactic disk, and to the nucleosynthesis in general are expected by comparing the observed abundances of oxygen isotopes with predictions of chemical evolution models based on more accurate oxygen yields.

Acknowledgements. We are indebted to Maria Lugaro and Paola Marigo for their careful reading of the manuscript, comments, and suggestions. We thank Thomas Lebzelter, Carlos Abia, Inma Dominguez, and Marco Limongi for the many helpful discussions about $^{16}O/^{17}O$ in RGB, AGB, and massive stars.

References

Abia, C., Palmerini, S., Busso, M., & Cristallo, S. 2012, A&A, 548, A55
Adelberger, E. G., García, A., Robertson, R. G. H., et al. 2011, Rev. Mod. Phys., 83, 195
Angulo, C., Arnould, M., Rayet, M., et al. 1999, Nucl. Phys. A, 656, 3
Boothroyd, A. I., Sackmann, I.-J., & Wasserburg, G. J. 1994, ApJ, 430, L77
Bruno, C. G., Scott, D. A., Aliotta, M., et al. 2016, Phys. Rev. Lett., 117, 142502
Buckner, M. Q., Iliadis, C., Kelly, K. J., et al. 2015, Phys. Rev. C, 91, 015812
Busso, M., Wasserburg, G. J., Nollett, K. M., & Calandra, A. 2007, ApJ, 671, 802
Busso, M., Palmerini, S., Maiorca, E., et al. 2010, ApJ, 717, L47
Charbonnel, C. 1995, ApJ, 453, L41
Charbonnel, C., & Lagarde, N. 2010, A&A, 522, A10
Charbonnel, C., & Zahn, J.-P. 2007, A&A, 467, L15
Chieffi, A., & Limongi, M. 2013, ApJ, 764, 21
Cristallo, S., Straniero, O., Piersanti, L., & Gobrecht, D. 2015, ApJS, 219, 40
Dearborn, D. S. P. 1992, Phys. Rep., 210, 367
Denissenkov, P. A., & Tout, C. A. 2003, MNRAS, 340, 722
Di Leva, A., Scott, D. A., Caciolli, A., et al. 2014, Phys. Rev. C, 89, 015803
Doherty, C. L., Gil-Pons, P., Lau, H. H. B., Lattanzio, J. C., & Siess, L. 2014, MNRAS, 437, 195
Eggleton, P. P., Dearborn, D. S. P., & Lattanzio, J. C. 2008, ApJ, 677, 581
El Eid, M. F. 1994, A&A, 285
García-Hernández, D. A., Lambert, D. L., Kameswara Rao, N., Hinkle, K. H., & Eriksson, K. 2010, ApJ, 714, 144
Gilroy, K. K., & Brown, J. A. 1991, ApJ, 371, 578
Gratton, R. G., Sneden, C., Carretta, E., & Bragaglia, A. 2000, A&A, 354, 169

Halabi, G. M., & Eid, M. E. 2015, MNRAS, 451, 2957
Harris, M. J., Lambert, D. L., & Smith, V. V. 1988, ApJ, 325, 768
Hinkle, K. H., Lebzelter, T., & Straniero, O. 2016, in AAS Meeting Abstracts, 227, 345.09
Iliadis, C., Longland, R., Champagne, A. E., Coc, A., & Fitzgerald, R. 2010, Nucl. Phys. A, 841, 31
Karakas, A. I., & Lattanzio, J. C. 2014, PASA, 31, e030
Karakas, A. I., Campbell, S. W., & Stancliffe, R. J. 2010, ApJ, 713, 374
Kobayashi, C., Karakas, A. I., & Umeda, H. 2011, MNRAS, 414, 3231
Langer, N., & Maeder, A. 1995, A&A, 295, 685
Lebzelter, T., Lederer, M. T., Cristallo, S., et al. 2008, A&A, 486, 511
Lebzelter, T., Straniero, O., Hinkle, K. H., Nowotny, W., & Aringer, B. 2015, A&A, 578, A33
Lederer, M. T., Lebzelter, T., Cristallo, S., et al. 2009, A&A, 502, 913
Limongi, M., Straniero, O., & Chieffi, A. 2000, ApJS, 129, 625
Limongi, M., Chieffi, A., & Straniero, O. 2001, Mem. Soc. Astron. It., 72, 289
Lodders, K. 2003, ApJ, 591, 1220
Lodders, K., Palme, H., & Gail, H.-P. 2009, in Landolt-Börnstein – Group VI Astronomy and Astrophysics, ed. J. E. Trümper, 4B, 4.4
Lugaro, M., Karakas, A. I., Bruno, C. G., et al. 2017, Nature Astron., 1, 0027
Nittler, L. R., & Gaidos, E. 2012, Meteor. Planet. Sci., 47, 2031
Nollett, K. M., Busso, M., & Wasserburg, G. J. 2003, ApJ, 582, 1036
Palacios, A., Charbonnel, C., Talon, S., & Siess, L. 2006, A&A, 453, 261
Palmerini, S., Busso, M., Maiorca, E., & Guandalini, R. 2009, PASA, 26, 161
Palmerini, S., La Cognata, M., Cristallo, S., & Busso, M. 2011, ApJ, 729, 3
Penzias, A. A. 1981, ApJ, 249, 518
Piersanti, L., Cristallo, S., & Straniero, O. 2013, ApJ, 774, 98
Prantzos, N., Aubert, O., & Audouze, J. 1996, A&A, 309, 760
Romano, D., & Matteucci, F. 2003, MNRAS, 342, 185
Scott, D. A., Caciolli, A., Di Leva, A., et al. 2012, Phys. Rev. Lett., 109, 202501
Siess, L. 2010, A&A, 512, A10
Smith, V. V., & Lambert, D. L. 1990, ApJS, 72, 387
Stancliffe, R. J. 2010, MNRAS, 403, 505
Stoesz, J. A., & Herwig, F. 2003, MNRAS, 340, 763
Straniero, O., Gallino, R., & Cristallo, S. 2006, Nucl. Phys. A, 777, 311
Straniero, O., Cristallo, S., & Piersanti, L. 2014, ApJ, 785, 77
Ventura, P., D'Antona, F., Di Criscienzo, M., et al. 2012, ApJ, 761, L30
Wouterloot, J. G. A., Henkel, C., Brand, J., & Davis, G. R. 2008, A&A, 487, 237